

**Photochemical Kinetic Modeling for Oxygen-enhanced UV-light-activated Corneal Collagen Crosslinking**

## ABSTRACT

**Aims:** To derive analytic formulas for the efficacy of type-II corneal collagen crosslinking (CXL) based on coupled macroscopic kinetic equations.

**Study design:** modeling and analysis of type-II CXL

**Place and Duration of Study:** New Vision Inc, Taipei, between Feb. 2017 and June 2017.

**Methodology:** Coupled macroscopic kinetic equations are derived under the quasi-steady state condition. The critical parameters influencing the efficacy of type –II CXL include: concentration and diffusion depth of the riboflavin,  $C(z,t)$ , and the oxygen  $[O_2]$ , the quantum yield, the UV light intensity ( $I_0$ ), dose and irradiation duration. Second-order solutions of  $C(z,t)$  and  $[O_2]$  are derived to calculate the type-II efficacy proportional to the time integration of  $C(z,t) [O_2]/([O_2]+b)$ . In the transient state with enough amount of oxygen, type-II process dominates over type-I. During the CXL, the oxygen profile is a decreasing function of time, UV light intensity and the stroma depth, where strong oxygen depletion (for high intensity) results a lower type-II efficacy.

**Conclusion:** Oxygen is not required in type-I CXL, whereas it is a must element in type-II CXL which has an efficacy is a nonlinear increasing function of the UV light dose (or fluence  $tI_0$ ), given by  $\ln [1+ Bt]$ , with B is proportional to  $C_0I_0$ . Type-II efficacy has an optimal dose, whereas type-I steady state efficacy is a decreasing function  $I_0$ .

**Keywords:** corneal crosslinking, CXL, efficacy, type-II, oxygen, kinetic modeling, ultraviolet light, riboflavin, photodynamic therapy

## 1. INTRODUCTION

Photochemical kinetics of CXL and the biomechanical properties of corneal tissue after CXL are reported [1]. However, much less efforts have been invested in basic theoretical studies of photopolymerization [2-13], where Lin et al presented the first dynamic modeling for the safety of CXL [2,3]. The safety and efficacy issues of CXL have been reported theoretically [4-6]. The critical parameters influencing the efficacy of corneal collagen crosslinking (CXL) include: initial concentration and diffusion depth of the riboflavin (for type-I CXL) and the oxygen (for type-II CXL), the quantum yield, the UV light intensity, dose and irradiation duration.

It has been reported that oxygen concentration in the cornea is modulated by UV irradiance and temperature and quickly decreases at the beginning of UV light exposure [9,14]. The oxygen concentration tends to deplete within about 10-15 seconds for irradiance of 3

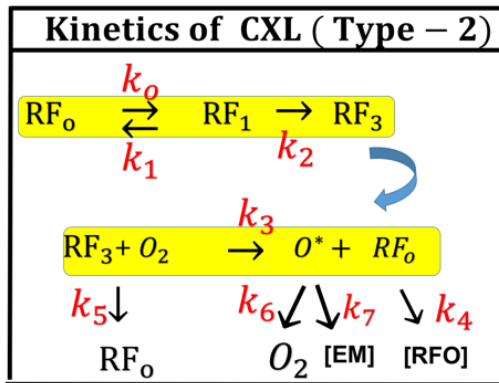
40 mW/cm<sup>2</sup> and within about 3-5 seconds for irradiance of 30 mW/cm<sup>2</sup> [9]. By using pulsed UV  
 41 light of a specific duty cycle, frequency, and irradiance, input from both Type I and Type II  
 42 photochemical kinetic mechanisms may be optimized to achieve the greatest amount of  
 43 photochemical efficiency. The rate of reactions may either be increased or decreased by  
 44 regulating one of the parameters such as the irradiance, the dose, the on/off duty cycle,  
 45 riboflavin concentration, soak time, and others [1,9].

46 The prior works of Zhu et al [7,8], Schumacher et al [9,10], and Kling [13] assumed a  
 47 constant UV light intensity and ignoring the RF depletion based on the conventional  
 48 Beer-Lambert law, underestimated the UV light intensity in the stroma during the CXL. The  
 49 prior work also assumed a flat RF concentration and ignored the absorption of the photolytic  
 50 products. Our model will remove all the above described oversimplified assumptions for a  
 51 much more realistic and accurate prediction of the key parameters influencing the CXL  
 52 efficacy. A generalized, time-dependent Beer-Lambert law is employed to solve the dynamic  
 53 UV light intensity [4,6]. The type-I efficacy (without oxygen) has been reported by Lin et al  
 54 [4,6], this study will focus on the oxygen-enhanced type-II efficacy

55 2. MATERIAL AND METHODS

56 2.1 The Modeling System

57



58

59 Fig. 1. The kinetics of type –II CXL. The ground state RF molecules [ $RF_0$ ] is excited by the  
 60 UV light to singlet excited state ( $RF_1$ ), and then triplet excited state ( $RF_3$ ). interacts with the  
 61 ground oxygen ( $O_2$ ) to form a reactive oxygen singlet (ROS),  $O^*$ . The ROS could be relaxed  
 62 to its ground state oxygen ( $O_2$ ), or interacts with the extracellular matrix (EM) to form cross  
 63 linking.

64

65 As shown in Fig. 1, the CXL type –II process is described as follows. The ground state RF  
 66 molecules is excited by the UV light to its singlet excited state ( $RF_1$ ), which could be relaxed  
 67 to its ground state or to a triplet excited state ( $RF_3$ ). In type-I process, ( $RF_3$ ) further interact  
 68 with the stroma collagen substrate for crosslinking. For type-II process, ( $RF_3$ ) interacts with  
 69 the ground oxygen ( $O_2$ ) to form a reactive oxygen singlet (ROS),  $O^*$ . The ROS could be

70 relaxed to its ground state oxygen (O<sub>2</sub>), or interacts with the extracellular matrix (EM) to kill  
 71 bacterial (to treat corneal ulcers) or to form cross linking.

72 The kinetic equations for the concentration of various components are shown by using  
 73 short-hand notations: C(z,t) and C\*(z,t) for the RF ground and singlet state [RF<sub>0</sub>] and [RF<sub>1</sub>];  
 74 X(z,t) and X\*(z,t) for the ground state [O<sub>2</sub>] and singlet oxygen [O\*<sub>2</sub>], T(z,t) for the RF triplet  
 75 state of [Rf3\*], and [EM] for the available extracellular matrix (EM); given by [6-9]

76

$$77 \quad \frac{\partial C(z,t)}{\partial t} = -k_0 C + k_1 C^* + k_3 X T - k_4 X^* C + k_5 T \quad (1.a)$$

$$78 \quad \frac{\partial C^*(z,t)}{\partial t} = k_0 C - k_1 C^* - k_2 C^* \quad (1.b)$$

$$79 \quad \frac{\partial T(z,t)}{\partial t} = k_2 C^* - k_3 X T - k_5 T \quad (1.c)$$

$$80 \quad \frac{\partial X(z,t)}{\partial t} = -P_1 \quad (1.d)$$

$$81 \quad \frac{\partial X^*(z,t)}{\partial t} = P_1 - k_4 X^* C - k_7 [EM] X^* \quad (1.e)$$

$$82 \quad \frac{\partial [EM]}{\partial t} = -k_7 X^* [EM] \quad (1.f)$$

83 where

$$84 \quad P_1 = a' I(z,t) k_3 X T - k_5 X^* \quad (1.g)$$

85

86 And the UV light intensity is given by

$$87 \quad \frac{\partial I(z,t)}{\partial z} = -A(z,t) I(z,t) \quad (2.a)$$

$$88 \quad A(z,t) = 2.3[(\varepsilon_1 - \varepsilon_2)X(z,t) + \varepsilon_2 X_0 F(z) + Q] \quad (2.b)$$

89

90  $a' = 83.6 p \varepsilon_1 \lambda$ , with p being the type-I quantum yield and  $\lambda$  being the UV light wavelength.;  
 91  $\varepsilon_1$  and  $\varepsilon_2$  are the extinction coefficients of RF and the photolysis product, respectively; Q is  
 92 the absorption coefficient of the stroma at the UV wavelength.

93 Time integration of the singlet oxygen concentration, or Eq. (1.f), efficacy of the type-II cross  
 94 linking given by the time integration of the singlet oxygen concentration. The normalized  
 95 efficacy of type-II cross linking defined by  $C_{eff} = 1 - [EM]/[EM]_0 = 1 - \exp(-S)$ , with S-function  
 96 given by [7,8]

$$97 \quad S = k_7 \int_0^t X^* dt \quad (3)$$

98 In the above described CXL model, the UV light intensity in the corneal stroma is given by a  
 99 time-dependent Beer-Lambert law [2,4,6]

$$100 \quad I(z, t) = I_0 \exp \left[ - \int_0^z A(z', t) dz' \right] \quad (4)$$

101 where the time-dependent extinction coefficient  $A(t)$  shows the dynamic feature of the UV  
 102 light absorption due to the RF concentration depletion. Without the RF,  $A(t)$  becomes a  
 103 constant given by the absorption coefficient of the corneal stroma tissue reported to be<sup>27</sup>  
 104  $A=2.3Q$ , with  $Q=13.9$  (1/cm). With the RF in the stroma, the initial (at  $t=0$ ) overall  
 105 absorption has an extra absorption defined by the extinction coefficient and initial  
 106 concentration of the RF, i.e.,  $A(z,t=0)=A_1=2.3 (Q + \varepsilon_1 C_0)$ , with the reported data [6,9]  $\varepsilon_1 =$   
 107  $204 (\% \cdot \text{cm})^{-1}$ . For  $t>0$ ,  $A(t)$  is an increasing function due to the deletion of RF in time and  
 108 defined by both the extinction coefficient of the RF ( $\varepsilon_1$ ) and its photolysis product ( $\varepsilon_2$ ),  
 109 where  $\varepsilon_2$  is not yet available for human, but was estimated to be about 50 to 120  $(\% \cdot \text{cm})^{-1}$ ,  
 110 based on measured data in RF solution under UV light irradiation[2,3]. The steady state light  
 111 intensity is given by the steady state absorption of  $A(z)=A_2= 2.3 (Q + \varepsilon_2 C_0)$ . We have  
 112 previously derived the effective intensity by its mean value using  $A(z,t) = 0.5 (A_1 + A_2)$ , or  
 113 using a numerically fit  $A(z,t)=2.3 (Q + m \varepsilon_2 C_0)$ , with fit parameter  $m=1.2$  to  $1.5$  for  $\varepsilon_2$  is 50  
 114 to 120  $(\% \cdot \text{cm})^{-1}$ . These methods provide us analytic formulas for the efficacy in type-I CXL  
 115 [4,6]. Similar approaches maybe used for type-II CXL as follows.

116 The kinetic equations (1) and (2) may be numerically calculated to find the CXL  
 117 efficacy, which however is too complex for us to analyze the roles of each of the parameters.  
 118 For comprehensive modeling we will use the so-called quasi-steady state assumption  
 119 described as follows. The life time of the singlet and triplet states of photosensitizer ( $C^*$  and  
 120  $T$ ) and the singlet oxygen ( $X^*$ ) are very short (ns to  $\mu\text{s}$  time scale) since they either decay or  
 121 react with cellular matrix immediately after they are created. Thus, it is reasonable is to set  
 122 the time dependences,  $dC^*/dt=dT/dt=dX^*/dt=0$ , or the quasi-steady-state conditions  
 123 introduced by Zhu et al. [7,8] in a different medical system. These conditions lead to the  
 124 macroscopic kinetic equation for the concentration of the ground state RF,  $C(z,t)$  and the  
 125 ground state oxygen,  $X(z,t)$ , as follows.

$$126 \quad \frac{\partial C(z,t)}{\partial t} = -KI(z,t)[1 + qH(z,t)]C(z,t) \quad (5.a)$$

$$127 \quad \frac{\partial X}{\partial t} = -bqKI(z,t)H(z,t) \quad (5.b)$$

$$128 \quad \frac{\partial I(z,t)}{\partial z} = -A(z,t)I(z,t) \quad (5.c)$$

$$129 \quad H(z,t) = C(z,t)X(z,t)/[X(z,t) + k] \quad (5.d)$$

130

131 where  $K = 83.6 \varepsilon_1 \lambda p$ ;  $\lambda$  is the UV light wavelength;  $p$  and  $q$  are the type-I and type-II

132 quantum yield, respectively, given by  $p = k_2/(k_1+k_2)$  and  $q = (k_3 - k_4)/(k_6+k_7[EM])$ ;  $k = k_5/k_3$ ,  $b =$   
 133  $k_7[EM]/(k_4 - k_5)$  having a typical value 1000 to 1500. Eq. (3) has been generalized for the  
 134 situation that both type-I and type-II CXL occur. It reduces to type-I only, when  $q=0$ , or  
 135  $dX/dt=0$ , or there is no oxygen supply in the process.

136 The initial concentration profiles (at  $t=0$ ) of the RF and oxygen may be calculated or  
 137 measured based on Fick's second law of diffusion [9,10,14]. For analytic solution, we have  
 138 chosen the distribution profile given by [3,6]:  $F(z,D) = 1 - 0.5z/D$  for RF solution, or  
 139  $C(z,t=0) = C_0F(z)$ , with a diffusion depth  $D$  in the stroma; and  $F'(D',z) = 1 - 0.5z/D'$  for the  
 140 oxygen, or  $X(z,0) = X_0F'(D',z)$ , with a different diffusion depth  $D'$ . The typical diffusion  
 141 depths are:  $D$  is 300 to 500  $\mu m$  and  $D'$  is 100 to 200  $\mu m$ .

142

143 The prior work of Zhu et al [7,8], Schumacher et al [9,10], and Kling [13] assumed a constant  
 144 UV light intensity and ignoring the RF depletion, i.e.,  $X(z,t) = X_0$ , is a constant in Eq. (2.b),  
 145 based on the conventional Beer-Lambert law which overestimated the  $A(z,t)$  as its initial  
 146 value when  $t > 0$ . The prior work also assume a flat RF concentration, or  $F(z,t) = 1$  and used an  
 147 oversimplified model to assume no absorption of the photolytic products, or  $\epsilon_2 = 0$ . Therefore,  
 148 our model system based on Eq. (1) and (2), is much more realistic than the prior works using  
 149 oversimplified assumptions.

150

## 151 2.2 Analytic Formulas

152 We will first derive the analytic formulas for the efficacy of type-II CXL (without the type-I),  
 153 we approximate  $H(z,t) = C(1-k/X)/k_3$ , such that the first-order solution (with  $k/X \ll 1$ ), of Eq.  
 154 (5.b) is given by the solution of  $dX/dC = b/X$ , or

155

$$156 \quad X(z,t) = X_0F'(z) - b \ln[C_0/C(z,t)] \quad (6)$$

157 Using the first-order solution of  $C(z,t)$  in Eq. (6), we find the second-order solution of Eq.

158 (5.a) and (5.b) for the oxygen,  $X(z,t)$ , and RF concentration,  $C(z,t)$  given by

$$159 \quad X(z,t) = X_0F'(z) - b \ln[1 + Bt] \quad (7.a)$$

$$160 \quad C(z,t) = C_0F(z)/[1 + Bt] \quad (7.b)$$

$$161 \quad B(z,t) = 1 - k'[1 - k'V(z,t)] \quad (7.c)$$

$$162 \quad V(z,t) = \ln[1 + B't] \quad (7.d)$$

163 with  $k' = k/X_0$ ,  $B'(z,t) = (1-k')apqI'(z)C_0F(z)$ . where we have used the mean intensity

164  $I'(z) = I_0 \exp(-A'z)$ , with  $A'$  is the fit steady-state value of  $A(z,t)$ , or its mean value,  $A' = 0.5(A_1$   
 165  $+ A_2)$  as defined earlier.

166 Therefore, the second-order quasi-steady state of the singlet oxygen,  $X^* = (apq/k_4)I'(z)H(z,t)$ ,  
 167 is approximated by the Eq. (7) and its time integration, from Eq. (3), gives the S function

168

$$169 \quad S(z,t) = (k_7/k_4)b_1V(z,t)[1 - b_2V(z,t)] \quad (8)$$

170

171 where  $b_1=1-k/X_0$ ,  $b_2=0.5kb/[apqI'(z)X_0^2]$ .

172 We note that  $S(z,t)$  has an optimal calculated by  $dS/dV=0$ , to obtain an optimal dose given by  
 173  $\ln(1+B't)=1/b_2$ .

174 For more complex case that both type-I and type-II coexist in the process, analytic formulas  
 175 are also available, when  $q/k_3 \ll 1$ , that is type-I is the dominant process. Using the similar  
 176 approach in type-II only situation, we obtain the second-order solution

177

178  $C(z,t) = C_0 F(z) \exp[-B''(z)t]$  (9.a)

179  $B''(z) = KI'(z) + K'(q/t)C_0 F(z)E'$  (9.b)

180  $E'(z,t) = 1 - \exp[-KI'(z)t]$  (9.c)

181 where  $K'=(1-k')/k_3$ . For the special case when  $q=0$ , or only type-I process, Eq. (9.a) reduces to  
 182 our previous formula. Using Eq. (9), we may solve for the oxygen concentration

183

184  $X(z,t) = X_0 F'(z) - b \ln[(1 + K'qC_0)/(1 + K'qC(z,t))]$  (10)

185 However, there is no analytic solution for the overall efficacy when type-I and type-II  
 186 coexist.

187 Comparing to the type-II  $S$  function in Eq. (8), the type-I efficacy  $C_{eff}(I)=1-\exp(-S')$ , with  
 188  $S'$  function given by [4,6]

189

190  $S'(z,t) = P(z,t) \sqrt{4KC_0 F(z)/(aI'(z))}$  (11.a)

191  $P(z,t) = 1 - \exp[-0.5atI'(z)]$  (11.b)

192

193 which is derived from the type-I rate equation of formation of polymers from the monomers,  
 194  $[M]$ , given by [6,11]

195

196  $\frac{\partial [M](z,t)}{\partial t} = -R(z,t)[M]$  (12.a)

197  $R(z,t) = \sqrt{a'KC(z,t)I(z,t)}$  (12.b)

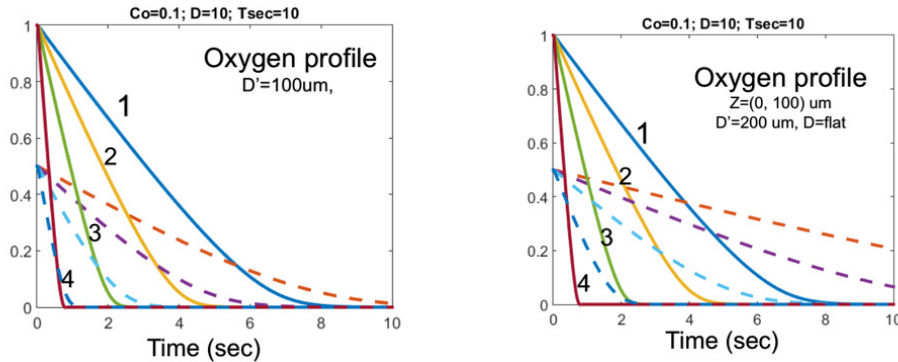
198 and  $S'$  is given by the time integration of  $R(z,t)$ .

199

200 **2. RESULTS**

201 The following calculations are based on the numerical solutions of Eq. (5) with input  
 202 parameters of:  $p=q=0.316$ , (or  $pq=0.1$ ),  $b=1000$ ,  $k=1.0$ ; initial RF concentration  $C_0 =0.1$ ,  
 203 oxygen concentration  $X_0=10$  mg/L. As shown by Fig. 1, the normalized oxygen profiles at  
 204  $z=0$  and 100  $\mu\text{m}$ , for various UV light intensity of (3,5,10,30)  $\text{mW}/\text{cm}^2$ , and oxygen initial  
 205 diffusion depth of  $D'=(100, 200)$   $\mu\text{m}$ . As predicted by Eq. (7.a), the oxygen concentration  
 206  $[O_2]$  is a decreasing function of time and depth ( $z$ ), but it is an increasing function of the

207 oxygen concentration diffusion depth ( $D'$ ). It is also a strong decreasing function of the UV  
 208 light intensity, in consistent with the clinically measured data. [ ]. It should be noted that  
 209 our modeling data has the similar trend as that of Kling [13], which, however, is not as  
 210 accurate as ours due to their simplified assumption of constant RF concentration in the  
 211 Beer-Lambert law, or  $A(z,t)$  in Eq. (2.b) is time-independent.  
 212



213  
 214 Fig. 2. The normalized oxygen profiles at  $z=0$  (solid curves) and 100  $\mu\text{m}$  (dashed curves), UV  
 215 light intensity of (3,5,10,30)  $\text{mW}/\text{cm}^2$  (curves 1,2,3,4); and oxygen initial diffusion depth ( $D'$ )  
 216 of 100  $\mu\text{m}$  (left figure) and 200  $\mu\text{m}$  (right figure), for initial RF flat distribution (or  $F=1.0$ ).  
 217

218 From Eq. (7) to Eq. (12), the key features of type-I and type-II are summarized and  
 219 compared as follows:

- 220 (a) In both type-I and type-II, the RF concentration is depleted by the UV light dose, but they  
 221 have different functional form, given by Eq. (6) and Eq. (9).
- 222 (b) In the transient stage with enough amount of oxygen, type-II process dominates over  
 223 type-I, whereas type-I becomes the dominating process after oxygen is depleted and  
 224 converted to the singlet oxygen. As shown by Eq. (8), the type-II efficacy is proportional  
 225 to  $Bt$ , or the products of the quantum yield ( $pq$ ), and the RF initial concentration,  $C_0F(z)$ .
- 226 (c) Both type-I and type-II efficacies are nonlinear increasing function of the UV light dose  
 227 (or fluence) in the transient state.
- 228 (d) At steady-state, type-I efficacy is a decreasing function of UV light intensity and the  
 229 corneal thickness, as shown by Eq. (11); whereas type-II has different dependence to the  
 230 UV light dose, having an optimal dose with steady state efficacy being a decreasing  
 231 function of light dose.
- 232 (e) The type-I efficacy is reduced by the type-II quantum yield ( $q$ ) when type-II co-exists.  
 233 Depletion of the RF concentration is much higher in type-I than type-II which as shown  
 234 by Eq. (5.a) with is proportional to  $(pq)$  having a value about 0.1 to 0.2, whereas the  
 235 depletion of type-I is proportional to  $p$  (about 0.3 to 0.5). The conventionally believed no  
 236 depletion of RF in type-II process is not correct, specially when the type-II is mixed with

237 type-I.

238 (f) Oxygen is not required in type-I, whereas it is a must element in type-II, as shown by Eq.  
239 (5.b), (7.d) and Eq. (8),  $V(z)=0$ , when  $B(z)=0$ , or  $X_0=0$ .

240 (g) As shown by Fig. 2, the oxygen profile is a decreasing function of time, UV light  
241 intensity, and the stroma depth ( $z$ ). Strong oxygen depletion (in high UV intensity) results  
242 a lower type-II efficacy.

243

#### 244 **4. CONCLUSION**

245 We have present the analytic formulas for type-II CXL efficacy based on coupled  
246 macroscopic kinetic equations. In the transient stage with enough amount of oxygen, type-II  
247 process dominates over type-I. The oxygen profile is a decreasing function of time, UV light  
248 intensity, and the stroma depth ( $z$ ). Strong oxygen depletion (in high UV intensity) results a  
249 lower type-II efficacy. Oxygen is not required in type-I, whereas it is a must element in  
250 type-II CXL which has an efficacy is a nonlinear increasing function of the UV light dose (or  
251 fluence  $tI_0$ ), given by  $\ln [1+ Bt]$ , with  $B$  is proportional to  $C_0I_0$ . Type-II efficacy has an  
252 optimal dose, whereas type-I steady state efficacy is a decreasing function  $I_0$ .

253 This article focuses on the analytic formulas and the features derived from them. Greater  
254 details of the roles of each of the parameters of  $[p,q,k,b,I, D.D']$  on the type-II efficacy  
255 require numerical simulation of Eq. (5), which will be presented elsewhere. The formulas  
256 developed in this study provide guidance for further clinical studies. The features predicted in  
257 this study is based on a modeling system which may not represent a real system. Moreover,  
258 parameters used in the calculatuons would require further clinical measurement for more  
259 accurate values.

#### 260 **CONSENT**

261 It is not applicable.

#### 262 **ETHICAL APPROVAL**

263 It is not applicable.

#### 264 **REFERENCES**

265

- 266 1. .Hafezi F and Randleman JB. editors. Corneal Collagen Cross-linking, second ed.  
267 Thorofare (NJ): SLACK; 2017.
- 268 2. Lin JT, Liu HW, Cheng DC. On the dynamic of UV-Light initiated corneal cross-linking.  
269 J. Med Biolog Eng. 2014;34:247-250; doi: 10.5405/jmbe.15332.
- 270 3. Lin JT, Cheng DC, Chang C, Yong Zhang. The new protocol and dynamic safety of  
271 UV-light activated corneal collagen cross-linking. Chinese J Optom Ophthalmol Vis Sci.  
272 2015;17:140-147.



- 273 4. Lin JT. Combined analysis of safety and optimal efficacy in UV-light-activated corneal  
274 collagen crosslinking. *Ophthalmology Research*. 2016; 6(2):1-14.
- 275 5. Lin JT. Efficacy and  $Z^*$  formula for minimum corneal thickness in UV-light crosslinking.  
276 *Cornea*. 2017 (in press).
- 277 6. Lin JT, Cheng DC. Modeling the efficacy profiles of UV-light activated corneal collagen  
278 crosslinking. *PloS One*. 2017;12:e0175002.
- 279 7. Zhu TC, Finlay JC, Zhou X, et al. Macroscopic Modeling of the singlet oxygen  
280 production during PDT. *Proc SPIE*. 2007; 6427:6427O81–6427O812.
- 281 8. Wang KKH, Finlay JC, Busch TM, et al. Explicit dosimetry for photodynamic therapy:  
282 macroscopic singlet oxygen modeling. *Journal of Biophotonics*. 2010; 3(5-6):304–318.  
283 [PubMed: 20222102].
- 284 9. Kamaev P, Friedman MD, Sherr E, Muller D. Cornea photochemical kinetics of corneal  
285 cross-linking with riboflavin. *Vis. Sci*. 2012;53:2360-2367.
- 286 10. Schumacher S, Mrochen M, Wernli J, Bueeler M, Seiler T. Optimization model for  
287 UV-riboflavin corneal cross-linking. *Invest Ophthalmol Vis Sci*. 2012;53:762-769.
- 288 11. Semchishen A, Mrochen A, Semchishen V. Model for optimization of the UV-A/Riboflavin  
289 strengthening (cross-linking) of the cornea: percolation threshold. *Photochemistry and*  
290 *photobiology*, 2015; 91:1403-1411.
- 291 12. Caruso C, Epstein RL, Ostacolo C, et al. Customized cross-linking- A mathematical model.  
292 *Cornea*, 2017; 36:600-604.
- 293 13. Kling S, Hafezi F. An algorithm to predict the biomechanical stiffening effect in corneal  
294 cross-linking. *J Refract Surg* 2017; 32:128-136.
- 295 14. Kling S, Richo O, Hammer A, et al. Increased biomechanical efficacy of corneal  
296 cross-linking in thin corneas due to higher oxygen availability. *J Refract Surg*.  
297 2015;31:840–846.